

# DRAFT JRC2015-5685

## EVALUATION OF LABORATORY AND FIELD EXPERIMENTATION CHARACTERIZING CONCRETE CROSSTIE RAIL SEAT LOAD DISTRIBUTIONS

**Matthew J. Greve, Marcus S. Dersch, J. Riley Edwards, and Christopher P. L. Barkan**

University of Illinois at Urbana-Champaign  
 Department of Civil and Environmental Engineering  
 Rail Transportation and Engineering Center (RailTEC)  
 205 N Mathews Ave  
 Urbana, IL, United States 61801

### ABSTRACT

As higher demands are placed on North American railroad infrastructure by heavy haul traffic, it is increasingly important to understand the factors affecting the magnitude and distribution of load imparted to concrete crosstie rail seats. The rail seat load distribution is critical to the analysis of failure mechanisms associated with rail seat deterioration (RSD), the degradation of the concrete surface at the crosstie rail seat. RSD can lead to wide gauge, cant deficiency, and an increased risk of rail rollover, and is therefore of primary concern to Class I Freight Railroads in North America. Researchers at the University of Illinois at Urbana-Champaign (UIUC) have successfully characterized the loading environment at the rail seat using matrix-based tactile surface sensors (MBTSS). Previous research has proven the feasibility of using MBTSS in both laboratory and field applications, and recent field experimentation has yielded several hypotheses concerning the effect of fastening system wear on the rail seat load distribution. This paper will focus on the analysis of data gathered from laboratory experimentation with MBTSS to evaluate these hypotheses, and will propose a metric for crosstie and fastening system design which considers the uniformity of the load distribution. The knowledge gained from this experimentation will be integrated with associated research conducted at UIUC to form the framework for a mechanistic design approach for concrete crossties and fastening systems.

### INTRODUCTION

As the demand in North America for high-performance, low-maintenance railroad infrastructure continues to increase, concrete crossties and elastic fastening systems are becoming increasingly common. Concrete crossties are typically used in areas of high curvature and steep grades on lines that

experience high-speed or heavy-axle load traffic [1]. Because of the increasingly common application of concrete crossties and elastic fastening systems in these high-demand environments, it is important to understand the factors contributing to common performance failures of concrete crossties and fastening systems. One of the most common failures of concrete crossties is the degradation of the concrete material directly below the rail, in the area of the crosstie known as the rail seat. This degradation is commonly referred to as rail seat deterioration (RSD), or rail seat abrasion (RSA). Figure 1 illustrates a typical instance of RSD, with the depth of wear increasing towards the field side of the rail seat. RSD has become a problematic failure for concrete crossties since it was first observed in the 1980's, and is often found in regions of steep grades, high curvature, and the presence of moisture [1]. If left untreated, RSD may lead to accelerated wear of the fastening system, wide gauge, excessive rail cant, and an increased risk of derailment due to rail rollover [1].



Figure 1. Typical Rail Seat Deterioration (RSD) Wear Pattern

According to a survey of North American railroad industry representatives, RSD is considered the most critical problem with concrete crossties and fastening systems. Additionally, it was ranked as the area of crosstie and fastening system research most in need of research [2]. As part of a larger research

project funded by the Federal Railroad Administration (FRA) investigating common failures with concrete crossties and elastic fastening systems, researchers at the University of Illinois at Urbana-Champaign (UIUC) are investigating the failure modes associated with RSD. Previous research has identified five failure mechanisms that may result in RSD: abrasion, crushing, freeze-thaw cracking, hydro-abrasive erosion, and hydraulic pressure cracking [1]. Of these five failure mechanisms, four are affected by the distribution of load at the crosstie rail seat, the exception being freeze-thaw cracking. Therefore, researchers at UIUC have undertaken an effort to better understand the distribution of the rail seat load, the factors that affect it, and its effect on rail seat deterioration. Previous research has highlighted the effect of pad modulus, fastening system type, loading environment, and RSD on the rail seat load distribution [3, 4, 5]. Researchers at UIUC hope to incorporate the findings on RSD failure mechanisms with other FRA-funded research to generate a framework for the mechanistic design of concrete crossties and their fastening systems, in which components are designed from expected outputs and observed relationships. It is believed that such a design approach would establish a clearer procedure for designing crossties and fastening systems, resulting in fewer service failures and higher reliability of the track structure and its components [6].

### INSTRUMENTATION TECHNOLOGY

To characterize the distribution of load at the crosstie rail seat, researchers at UIUC have utilized matrix-based tactile surface sensors (MBTSS). The MBTSS system used by UIUC is manufactured by Tekscan® Inc. and consists of rows and columns of conductive ink which, when pressed together by a load applied normal to the contact plane, output a change in resistivity at each intersection of a row and a column. This output, termed a “raw sum”, can be interpreted as the pressure exerted on the sensor at a given intersection when given the total applied load. MBTSS simultaneously outputs the area over which this load is applied. This is termed the “contact area” of the load and is calculated from the number of sensing locations that indicate an applied load. Data is collected from the entire sensing area at a maximum rate of 100 Hz. The data is calibrated during analysis using a known or assumed input load.

Previous experimentation at the University of Kentucky (UK) and UIUC have shown that MBTSS are susceptible to shear and puncture damage. To protect the sensors, layers of biaxially-oriented polyethylene terephthalate (BoPET) and polytetrafluoroethylene (PTFE) are secured to both sides of a sensor that has been trimmed to fit the rail seat. The assembly is then installed between the rail pad assembly and the concrete crosstie rail seat (Figure 2) [7].

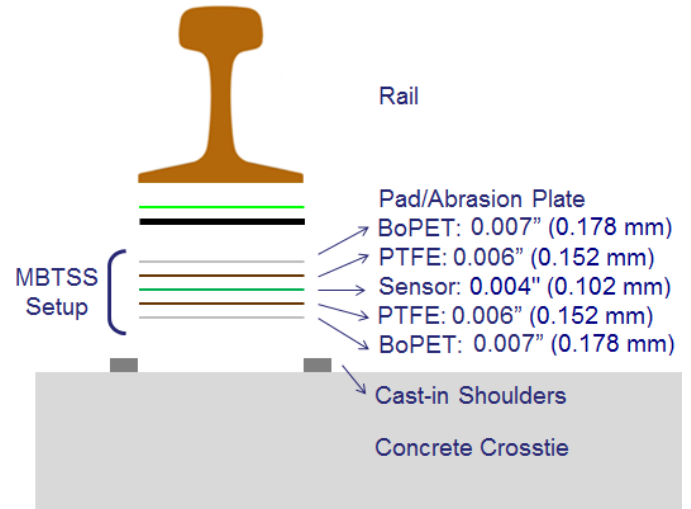


Figure 2. MBTSS Layers and Thicknesses [7]

### FIELD INSTRUMENTATION

Field experimentation was performed at the Transportation Technology Center (TTC) in Pueblo, Colorado, USA, a research and testing facility that consists of 48 miles (77.2 km) of railroad track with variable geometries and operating conditions. A section of 15 concrete crossties with Safelok I shoulders was installed on the 13.5 mile (21.7 km) Railroad Test Track (RTT) in a section of tangent track. Eight rail seats, on five crossties, at this site were instrumented with MBTSS (Figure 3). Five consecutive rail seats were chosen in an attempt to fully capture the vertical load distribution, and to investigate the effect and variability of support conditions in a group of crossties. Additionally, three consecutive rail seats on the opposite rail were selected to provide further information on load transfer, and to examine the variability of support conditions across a single crosstie.

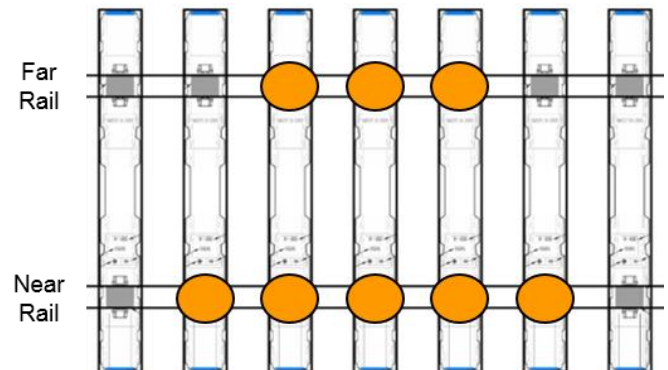


Figure 3. Plan View of MBTSS Field Installation at TTC

Although the rail pad assemblies and insulators were replaced prior to field experimentation, the clips were not. At the time of experimentation, the clips had been subjected to 5 million gross tons (MGT) of traffic and 3 cycles of removal and

reapplication. It was hypothesized that the wear on the fasteners, especially due to the 3 reapplications, significantly reduced the applied toe load. This reduced the ability of the fastening system to resist rail rotation under lateral load, which has been shown to lead to significant rail seat load concentrations [6].

## LABORATORY INSTRUMENTATION

Laboratory experimentation was performed at the Research and Innovation Laboratory (RAIL) at Schnabel, a facility owned by UIUC for research on and testing of railroad infrastructure systems and components. Experiments were conducted using the Track Loading System (TLS), a loading frame which can accommodate a 22 foot (6.7 m) section of track with full depth substructure (Figure 4). A track segment of 11 concrete crossties with Safelok I shoulders was constructed to Class I specifications and instrumented to replicate field conditions. Five consecutive rail seats on the TLS were instrumented with MBTSS to fully capture the vertical load distribution and investigate the variability of support conditions (Figure 5).



Figure 4. Track Loading System (TLS) Installation during Experimentation

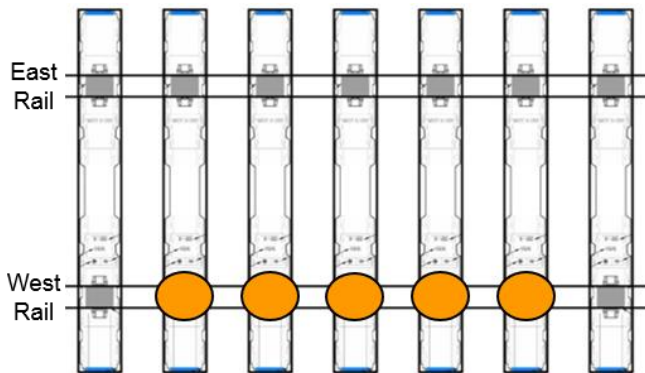


Figure 5. Plan View of MBTSS Lab Installation on the TLS

During laboratory experimentation, any clips that were removed were replaced with new clips to maintain an unworn condition. Although other sources of variation exist between the TLS and the RTT, it is believed that the health of the fastening system had the greatest effect of the possible variables between laboratory and field rail seat load distribution results for identical loading environments.

## EXPERIMENTATION LOADING ENVIRONMENT

The application of loads during field experimentation was accomplished using the Track Loading Vehicle (TLV). The TLV is owned by the Association of American Railroads (AAR) and operated by the Transportation Technology Center, Inc. (TTCI). The TLV can be used to study a variety of applications including wheel climb derailments, vertical modulus, lateral track strength, gage widening, and wheel/rail force relationships [8]. An instrumented wheelset is attached to vertically- and laterally-oriented actuators, which are attached to the frame of a modified rail car. The TLV's ability to apply controlled vertical and lateral loads to the rail using realistic loading conditions and application made it an ideal tool for the purposes of this experimentation.

The application of loads during laboratory experimentation was accomplished using the TLS. For this experimentation, vertical loads were applied using two hydraulic actuators, and the lateral loads were applied using a single manually-operated hydraulic jack (Figure 4). The vertical loads were applied to both journals of a standard 36 inch (91.4 cm) wheelset through standard journal adaptors, and the lateral loads were applied towards the West (instrumented) Rail.

The testing procedure in both the field and the lab consisted of applying loads to both rails with the loading axle centered above each instrumented crosstie. Vertical loads were applied to each rail at increasing magnitudes from 0 to 40 kip (178 kN) at 5 kip (22.2 kN) increments. In the field, gauge-widening lateral forces were applied at a 20 kip (88.9 kN) vertical load, resulting in L/V force ratios ranging from 0.0 to 0.6 at 0.1 increments, and at a 40 kip (178 kN) vertical load, resulting in L/V force ratios ranging from 0.0 to 0.5 at 0.1 increments, followed by a final increment of 0.05, resulting in a final L/V force ratio of 0.55. In the lab, lateral forces were applied at 10 kip (44.5 kN), 20 kip (88.9 kN), 30 kip (133 kN), and 40 kip (178 kN) vertical loads, resulting in L/V force ratios ranging from 0.0 to 0.6 at 0.1 increments at all four vertical loads.

## RESULTS

Figure 6 compares the qualitative effect of lateral to vertical (L/V) force ratio under a constant 40 kip (178 kN) vertical load for three separate cases. The first case represents the common design assumption that the rail seat load is distributed uniformly across the entire rail seat. By definition, this distribution is not affected by L/V force ratio. The second

case represents a typical rail seat load distribution for a rail seat with new fasteners, as illustrated by data from experimentation on the TLS. Although there is some concentration of load on the field side of the rail seat, the fasteners are able to restrict rail rotation to 0.31 degrees or less. This results in very little change in rail seat load distribution. The final case represents a typical rail seat load distribution for a rail seat with worn fasteners, as illustrated by data from experimentation on the RTT using the TLV. The ability of the clips to restrict rail rotation is reduced, allowing rail rotations up to 0.52 degrees, which results in significant concentration of the rail seat load along the field side of the rail seat. Further, this excessive rail rotation results in a complete unloading of the gauge side of the rail seat at high L/V ratios. Figure 6 also shows the change in pressures exerted on the rail seat: the increased rail rotation in the worn fastener case results in higher pressures than the new fastener case, as illustrated by the accompanying pressure scale.

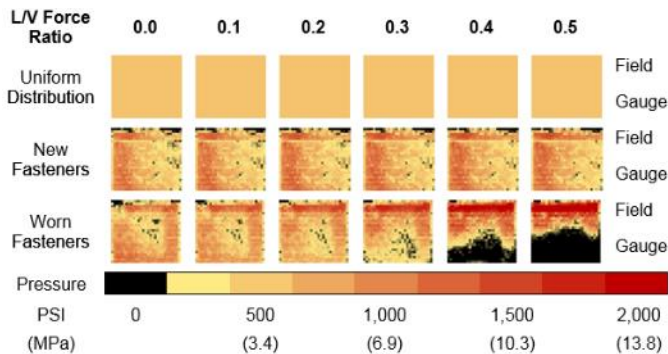


Figure 6. Rail Seat Load Distributions under 40 Kip (178 kN) Vertical Wheel Load at Varying L/V Force Ratios

Figure 7 illustrates the quantitative effect of L/V force ratio and fastener health on contact area, the area of the rail seat that is engaged in load transfer. The data has been normalized to the contact area seen under a 40 kip (178 kN) vertical and 0 kip lateral loading environment. Therefore, the percent of contact area at a 0.0 L/V force ratio describes the effect of vertical load, while the change in percent contact area for each data series describes the effect of L/V force ratio for each vertical load magnitude. The new fastener case results in a consistent increase in contact area for all vertical load magnitudes between 0.58% and 1.75%. It is hypothesized that this increase is due to deformation of the rail pad assembly as the rail rotates under higher L/V force ratios. By contrast, the worn fastener case exhibits a loss of up to 42% of initial contact area once the L/V force ratio exceeds a critical “threshold” value [4]. These data support the hypothesis that the ability of the worn fasteners to restrict rail rotation was reduced, which resulted in the observed lower contact areas under worn fasteners.

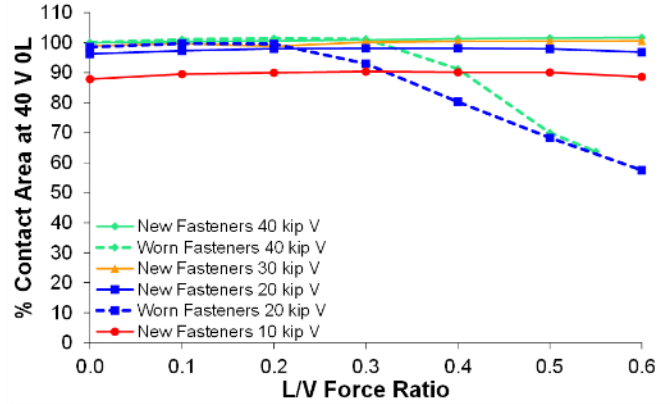


Figure 7. Effect of L/V Force Ratio on Contact Area

In order to examine the effect of fastener wear and loading environment on pressures, it is necessary to determine the total load applied to each rail seat. For the new fastening system investigated in the laboratory, the rail seat load was calculated from internal strain gauges embedded below the crosstie rail seat. For the worn fastener case (data collected in the field), these embedment gauges were not present on rail seats instrumented with MBTSS. It was therefore necessary to estimate the rail seat load directly below the point of loading. The rail seat load in this case was estimated to be half of the vertical wheel load, based on both an extensive literature review [6] and data acquired from strain gauges used in conjunction with field experimentation.

Figures 8 and 9 illustrate the effect of loading environment on the pressures exerted on the crosstie rail seat. There are three primary metrics used to characterize the pressures at the rail seat interface. The first is the theoretical uniform pressure, which represents conventional design methodology. It assumes that the rail seat load is evenly distributed across the rail seat and is not affected by L/V force ratio, analogous to the uniform pressure distribution case illustrated in Figure 6. The second is the average pressure, which is calculated by dividing the rail seat load by the measured contact area. The third pressure metric is the maximum pressure observed for a given combination of vertical load and L/V force ratio.

Figure 8 compares the uniform, average, and maximum pressures for the new and worn fastener cases under a 20 kip (88.9 kN) vertical load, and Figure 9 compares the uniform, average, and maximum pressures for the same cases under a 40 kip (178 kN) vertical load. In both figures, the new fastener average pressures plot within 50% of the theoretical uniform pressure, even under L/V force ratios as high as 0.6. This indicates that almost all of the contact area is utilized in load transfer. The worn fastening system average pressures plot close to the theoretical uniform pressure below the aforementioned “threshold” L/V force ratio.

Above this critical point, the reduction of contact area increases these pressures by up to 80% of their original value. The maximum pressures observed for the new fastener case were approximately 325% higher than the theoretical uniform

pressure under a 20 kip (88.9 kN) vertical wheel load, experiencing no net change from 0 to 0.6 L/V. Under a 40 kip (178 kN) vertical wheel load, the new fastener maximum pressures are inversely related to L/V force ratio, ranging from 211% to 177% higher than the theoretical uniform pressure. By contrast, the maximum pressures observed in the worn fastening system case for both vertical wheel load magnitudes exhibited strong positive correlation with L/V force ratio. Again, the magnitude of maximum pressure relative to the theoretical uniform pressure is greater under the 20 kip vertical load, ranging from 350% to 660% greater than the theoretical uniform pressure, than under the 40 kip vertical wheel load, ranging from 160% to 370% greater than the theoretical uniform pressure.

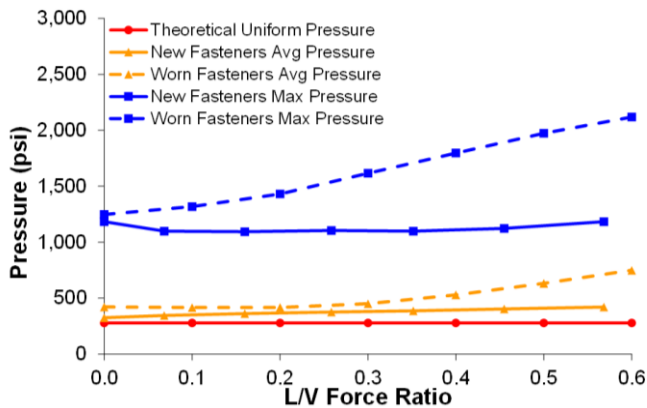


Figure 8. Effect of L/V Force Ratio on Pressure (20 Kip (88.9 kN) Vertical Wheel Load)

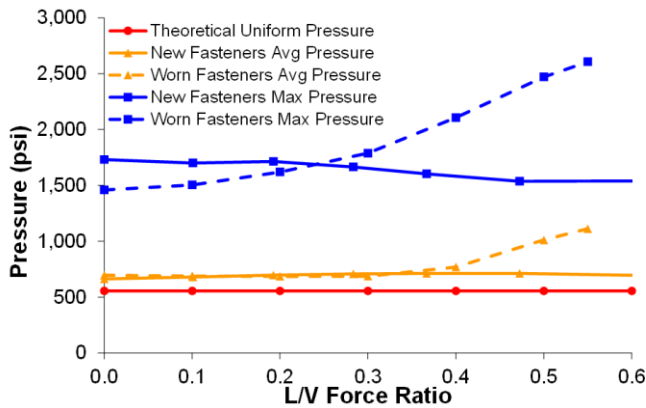


Figure 9. Effect of L/V Force Ratio on Pressure (40 Kip (178 kN) Vertical Wheel Load)

It is important to note that although none of the observed pressures approach the design compressive strength of the concrete (i.e. 7,000 psi [9]), the increase in pressure will change the characteristics of failure mechanisms associated with RSD (e.g. increased frictional force leading to more severe abrasion). It is hypothesized that RSD first develops in regions of extreme pressure and then spreads as the loss of material becomes more severe. Figure 9 shows a higher maximum pressure for the new

fastening system case than was observed in the worn fastener case under a 40 kip vertical wheel load. It is hypothesized that this is due primarily to increased rail seat load on the instrumented rail seats resulting from stiffer support conditions relative to adjacent crossies.

Analysis of the data presented in this paper has shown that fastener wear can lead to significant concentration of the rail seat load on the field side of the rail seat under high L/V force ratios. Figure 10 shows the distribution of rail seat load in the worn fastener case as a function of the distance from the field side shoulder. The data series were calculated by summing the load applied to each sensor row, which are 0.22 inches (5.59 mm) in width, at each L/V force ratio. As the L/V force ratio increases, the data show significant concentration of the rail seat load on the field side of the rail seat, and an unloading of the gauge side of the rail seat, which agrees with the analysis detailed in this report. The area of the rail seat 1 inch (25.4 mm) or less from the field side shoulder, illustrated by the area left of the dashed line in Figure 10, exhibits the highest sensitivity to changes in the L/V force ratio, and consistently exhibits significantly higher loads than the remainder of the rail seats. Figure 10 also shows the effect of the rail pad texture. The micro-level variations in each data series are due to studs on the bottom of the rail pad designed to allow water to drain from the rail pad-abrasion frame interface, with higher loads occurring under the studs. Although the variation in load due to rail pad texture are not as significant as those due to changes in the loading environment, it is interesting to note that the effect of rail pad texture does have a visible impact on the rail seat load distribution.

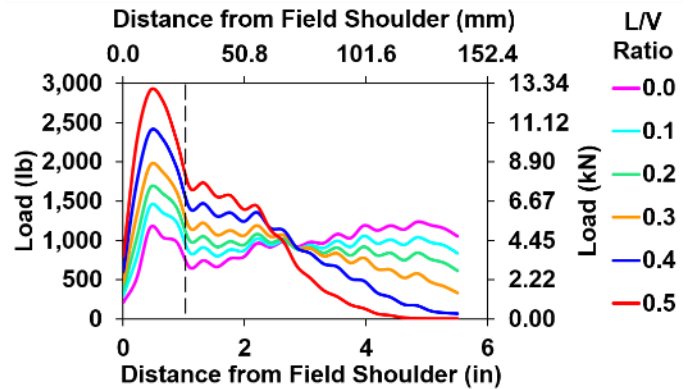


Figure 10. Lateral Distribution of Rail Seat Load at Varying L/V Force Ratio (40 Kip (178 kN) Vertical Wheel Load)

### RAIL SEAT LOAD INDEX (RSLI) DESIGN METRIC

The Rail Seat Load Index (RSLI) is proposed as a quantifiable design value which describes the sensitivity of the rail seat load distribution to changes in the L/V force ratio. The RSLI of a rail seat describes the portion of the total rail seat load that is imparted onto a critical region of the rail seat, normalized to a theoretical uniform distribution, as described in

Equation 1. Because the RSLI is calculated from a ratio of loads, RSLI can be applied to any units of load, provided that the same units are used for both the vertical load applied to the critical area and the total vertical rail seat load. This critical region is defined as the area of the rail seat not more than 1 inch (25.4 mm) from the field side shoulder. Field experimentation has shown that this region of the rail seat is the most sensitive to changes in the L/V force ratio (Figure 10). Therefore, for a 6 inch (152.4 mm) rail base, one sixth of the total rail seat load will be imparted onto the critical region in the theoretical uniform loading case.

$$\begin{aligned}
 RSLI &= \frac{\frac{[Load\ in\ Critical\ Area]}{[Total\ Rail\ Seat\ Load]}}{1/6} \\
 &= 6 * \frac{[Load\ in\ Critical\ Area]}{[Total\ Rail\ Seat\ Load]} \quad (1)
 \end{aligned}$$

To further explain this metric, RSLI values can be calculated for the data presented in this paper (Figure 11). The average effect of increasing L/V force ratio on RSLI for both the new and worn fastener cases are shown for a 40 kip (178 kN) vertical wheel load. At a 0.0 L/V force ratio, both the new and worn fastener cases achieve an RSLI near 1, indicating a proportionate amount of the rail seat load is imparted to the critical area. The new fastener RSLI increases to 1.4 at a 0.6 L/V force ratio; by Equation 1, this indicates that slightly less than one quarter of the total rail seat load is applied to the one inch closest to the field side shoulder. By contrast, the worn fastener case experiences a significant increase in RSLI, with a maximum RSLI of 3.1 at 0.55. By Equation 1, this means that more than half of the rail seat load is concentrated in the critical area of the rail seat, indicating a severely nonuniform load confirmed by the analysis detailed in this paper. Lastly, Figure 11 also includes RSLI data from joint experimentation with TTCI examining the effect of rail seat deterioration on the rail seat load distribution [5]. This data is representative of extreme RSLI that may occur in the field as a result of 0.75 inches (19.1 mm) of RSD: at 0.0 L/V, the data shows an RSLI of 2.8 and increases to 4.1 under a 0.6 L/V force ratio. This represents two thirds of the rail seat load applied to the one inch closest to the field side of the rail seat.

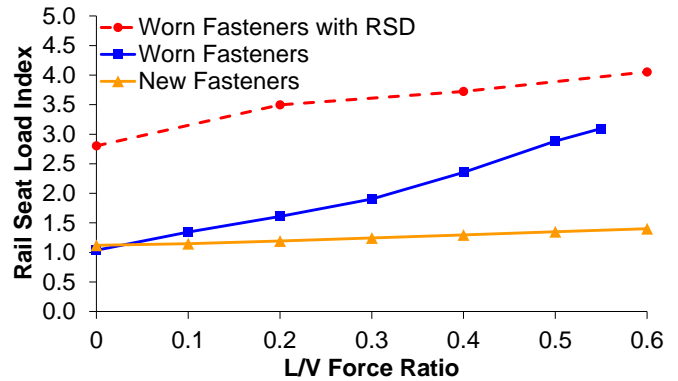


Figure 11. Effect of L/V Force Ratio on RSLI (40 Kip (178 kN) Vertical Wheel Load)

Although no criteria for maximum permissible RSLI has been established, it is theorized that a maximum RSLI exists which permits limited concentration of the rail seat load, but prohibits excessive loading on the field side of the rail seat. This would result in accelerated wear of the fastening system and an increased potential for RSD. Figure 12 illustrates this hypothetical range, which does not vary with L/V Force Ratio. Instead, the fastening system should be designed to meet the maximum permissible RSLI at the design L/V; this will result in stiffer fastening system designs for loading environments in which high L/V force ratios are common. Further, this allows for fastening systems to be optimized for their design application, rather than designing all fastening systems to the same standard regardless of application.

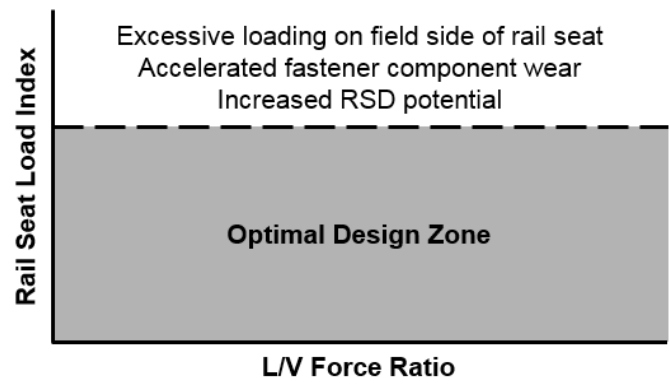


Figure 12. Conceptual RSLI Design Limit Philosophy

To determine the maximum RSLI of a fastening system, an experimental testing procedure has been developed. This RSLI test would be performed on a single rail seat in conjunction with AREMA Test 6 (Wear and Abrasion) to examine both new and worn fastening system component conditions. The test utilizes a loading frame capable of applying controlled vertical and lateral loads of independently varying magnitude to the rail head. A section of 136RE rail 18 inches (457 mm) in length should be affixed to a single rail seat with a typical fastening system, with MBTSS installed between the fastening system and crosstie rail seat (Figure 2). The assembly should

then be subjected to the design vertical load. Once the design vertical load is reached, the lateral load should be increased until the design L/V force ratio is achieved. MBTSS is then removed, and the same fastening system components are reassembled and subjected to AREMA Test 6. Following Test 6, the fastening system is disassembled, MBTSS is reinstalled, the fastening system is reassembled once more, and is then again subjected to the design loading environment. Failure criteria for the test would be established based on both the change in RSLI as a result of AREMA Test 6, and the absolute maximum RSLI recorded during the test.

## CONCLUSIONS AND FUTURE WORK

Data from this experimentation have shown that the health of the fastening system has a significant effect on the rail seat load distribution in concrete crossties. Data collected from laboratory experimentation on a track structure with new fasteners were compared to data from field experimentation under identical loading scenarios on a track structure with fasteners that had been subjected to both 5 MGT of traffic and, more importantly, 3 reapplication cycles. This wear on the fasteners resulted in an average reduction of contact area by 40%, an increase in average pressure by 71%, and an increase in maximum pressure by 60%, relative to the performance of new fasteners. Further, it was shown that under the worn fastener case, the portion of the rail seat load distributed within one inch of the field side shoulder was the most sensitive to changes in L/V force ratio, accounting for up to half of the total rail seat load under high L/V force ratios. It is therefore deemed important to consider the effect of fastening system wear when evaluating the long-term performance of concrete crossties and fastening systems. Further experimentation to quantify the effect of traffic on fastening system wear, and therefore rail seat load distribution, would therefore be beneficial to understanding the parameters critical to preventing RSD.

Current design methodology regards the rail seat load as uniformly distributed across the entire rail seat. As illustrated in this paper, however, this assumption does not accurately describe the behavior of the rail seat load at high L/V force ratios. Even under a healthy rail seat, the load distribution is nonuniform, and may experience maximum pressures twice as high as predicted by the theoretical uniform distribution of pressure. Higher pressures in crosstie design may affect the failure mechanisms associated with RSD. Therefore, a design check such as RSLI ensuring that the rail seat load distribution does not generate these critical higher pressures would lead to more optimal fastening system designs with a greater resistance to wear. A study comparing the RSLI of common fastening systems both in the new and worn case would further the understanding of the practical design zone for RSLI, and experimentation characterizing the relationship between RSD

failure mechanisms and rail seat load nonuniformity would aid in the development of mechanistic thresholds for RSLI.

Further, experimentation to establish a relationship between RSLI and a measurement presently obtained from AREMA Test 6 experiments would allow for more widespread adaptation of the concept behind RSLI without necessitating the acquisition of specialized instrumentation. Ultimately, the consideration of rail seat load nonuniformity in the design of concrete crossties and fastening systems will lead to designs with a greater inherent resistance to RSD.

## ACKNOWLEDGMENTS

This research was primarily funded by United States Department of Transportation (US DOT) Federal Railroad Administration (FRA). The first two authors were supported by a research grant from Amsted RPS. Additional support was provided by the National University Rail (NURail) Center, a US DOT-OST Tier 1 University Transportation Center. The published material in this report represents the position of the authors and not necessarily that of US DOT. Generous support and guidance has also been provided from the industry partners of this research: Union Pacific Railroad; BNSF Railway; National Railway Passenger Corporation (Amtrak); Amsted RPS / Amsted Rail, Inc.; GIC Ingeniería y Construcción; Hanson Professional Services, Inc.; and CXT Concrete Ties, Inc., and LB Foster Company. J. Riley Edwards has been supported in part by grants to the UIUC Rail Transportation and Engineering Center (RailTEC) from CN, CSX, Hanson Professional Services, and the George Krambles Transportation Scholarship Fund. For providing direction, advice, and resources, the authors would like to thank Christopher Rapp from Hanson Professional Services, Inc, Mauricio Gutierrez from GIC Ingeniería y Construcción, Professor Jerry Rose and Graduate Research Assistant Jason Stith from the University of Kentucky, and Vince Carrara from Tekscan®, Inc. The authors would also like to thank Marc Killion, Tim Prunkard, and Don Marrow from the University of Illinois at Urbana-Champaign for their assistance in laboratory experimentation, and undergraduate research assistants Douglas Capuder, Zachary Ehlers, Zachary Jenkins, and Daniel Rivi for their assistance in analyzing the data presented in this paper.

## REFERENCES

1. Zeman, J. C. Hydraulic Mechanisms of Concrete-Tie Rail Seat Deterioration. University of Illinois at Urbana-Champaign, Urbana, Illinois, M.S. Thesis 2010.
2. Van Dyk, B. J., M. S. Dersch, J. R. Edwards, C. J. Ruppert, Jr., and C. P.L. Barkan Load Characterization Techniques and Overview of Loading Environment in North America. Accepted *Transportation Research Record: Journal of the Transportation Research Board*, Transportation Research Board of the National Academies, Washington, D.C., 2014.
3. Rapp, C. T., M. S. Dersch, J. R. Edwards, C. P.L. Barkan, B. Wilson, and J. Mediavilla. Measuring Rail Seat Pressure Distribution In Concrete Crossties: Experiments with Matrix-Based Tactile Surface Sensors. In *Transportation Research Record: Journal of the Transportation Research Board*, No. 2374, Transportation Research board of the National Academies, Washington, D.C., 2014, pp. 190—200.
4. Greve, M., M. S. Dersch, J. R. Edwards, C. P.L. Barkan, J. Mediavilla, and B. Wilson. Analysis of the Relationship between Rail Seat Load Distribution and Rail Seat Deterioration in Concrete Crossties. In *ASME Joint Rail Conference*, Colorado Springs, Colorado, 2014.
5. Greve, M. J., M. S. Dersch, J. R. Edwards, C. P.L. Parkan, H. Thompson, T. Sussman, and M. McHenry. Examination of the Effect of Concrete Crosstie Rail Seat Deterioration on Rail Seat Load Distribution. Accepted *Transportation Research Record: Journal of the Transportation Research Board*, Transportation Research Board of the National Academies, Washington, D.C., 2015.
6. RailTEC. FRA Improved Concrete Crossties and Fastening Systems for US High Speed Passenger Rail and Joint Passenger/Freight Corridors. Railroad Transportation and Engineering Center (RailTEC), University of Illinois at Urbana-Champaign (UIUC), Urbana, Illinois, United States Department of Transportation (USDOT) Federal Railroad Administration (FRA) Final Report 2013.
7. Rapp, C. R., J. R. Edwards, M. S. Dersch, C. P.L. Barkan, B. Wilson, and J. Mediavilla. Measuring Concrete Crosstie Rail Seat Pressure Distribution with Matrix Based Tactile Surface Sensors. In *2012 ASME Joint Railroad Conference*, Philadelphia, PA, April 2012, pp. 2-3.
8. Schust, W. C., and J. A. Elkins. Wheel Forces During Flange Climb. In *IEEE/ASME Joint Railroad Conference*, Boston, MA, March 1997, pp. 137-147.
9. American Railway Engineering and Maintenance-of-Way Association. Manual for Railway Engineering. 2014.